Published in final edited form as:
ACS Chem Biol. 2019 June 21; 14(6): 1243–1248. doi:10.1021/acschembio.9b00205.

Polyanion-Assisted Ribozyme Catalysis Inside Complex Coacervates

Raghav R. Poudyal[1,3,*], **Christine D. Keating**[1,*], **Philip C. Bevilacqua**[1,2,3,*]

[1]Department of Chemistry, Pennsylvania State University, University Park, Pennsylvania, 16802, USA.

[2]Department of Biochemistry, Microbiology, and Molecular Biology, Pennsylvania State University, University Park, Pennsylvania, 16802, USA.

[3]Center for RNA Molecular Biology, Pennsylvania State University, University Park, Pennsylvania, 16802, USA.

Abstract

Owing to their ability to encapsulate biomolecules, complex coacervates formed by associative phase separation of oppositely-charged polyelectrolytes have been postulated as prebiotic non-membranous compartments (NMCs). Recent studies show that NMCs sequester RNA and enhance ribozyme reactions, a critical tenet of the RNA World Hypothesis. As RNA is negatively charged, it is expected to interact with polycationic coacervate components. The molecular basis for how identity and concentration of polyanionic components of complex coacervates affect ribozyme catalysis remains unexplored. We report here a general mechanism wherein diverse polyanions enhance ribozyme catalysis in complex coacervates. By competing for unproductive RNA-polycation interactions, polyanions enhance ribozyme reaction more than 12-fold. The generality of our findings is supported by similar behavior in three polyanions—polycarboxylates, polysulfates and polysulfates/carboxylates—and two different ribozymes, the hammerhead and hairpin. These results reveal potential roles for polyanions in prebiotic chemistry and extant biology.

Graphical Abstract

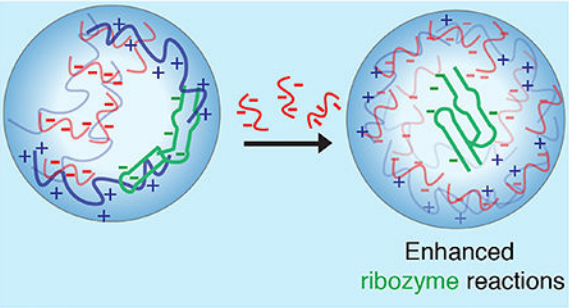

[*]Authors to whom correspondence should be addressed: rup34@psu.edu, keating@chem.psu.edu, pcb5@psu.edu.

Supporting Information Available: This material is available free of charge *via* the Internet

Introduction

Membraneless compartments called complex coacervates form by associative liquid-liquid phase separation (LLPS) of oppositely charged polyelectrolytes.[1] As complex coacervates form spontaneously, selectively encapsulate biomolecules[2, 3], and support biochemical reactions[4,5], they present simpler alternatives to membrane-bound protocells[6, 7]. Recent studies demonstrate that certain complex coacervates support non-enzymatic polymerization of RNA[8] and enhance ribozyme reactions[8, 9], chemistries potentially relevant to the origin and evolution of life[6]. Associative LLPS also forms non-membranous compartments (NMCs) in extant cells,[10] which partition RNAs and proteins.[11–13] For example, in the case of the nucleolus, LLPS has been hypothesized to regulate rRNA biogenesis by controlling transport and processing[14]. There is pressing need to uncover effects of constituent molecules on the biophysical and biochemical properties of membraneless compartments.[15, 16]

Cationic polyamines have been used to study complex coacervates[2, 4, 8, 9, 17] and polycation identity affects RNA chemistries;[8] however, effects of polyanions of complex coacervates on functional RNAs are relatively unexplored. We show herein that polyanions enhance ribozyme catalysis in coacervates by competing with inhibitory RNA-polycation interactions. We demonstrate that anion-assisted increase of ribozyme activity in complex coacervates is general and achievable by different polyanions. Our study reveals that optimal ribozyme activity may be attained by changing the size, identity, or amount of polyanions in complex coacervates. As such, it provides a guide to complex coacervate compositions that favor ribozyme reactions[18–21] relevant to origin of life scenarios.

Results and Discussion

First, we investigated effects of polyanion multivalency on complex coacervate-mediated enhancements of ribozyme reactions, using the two-piece hammerhead ribozyme (Figure 1A). Poly(diallyldimethylammonium chloride) (PDAC) with 53 monomers and oligoaspartic acids (D_n) with 10, 30, 50, and 100 monomers were chosen as polycation and polyanions, respectively to generate complex coacervates (Figure 1B and C, Supplementary Table 1). The dissociation constant between the enzyme (2.5 nM) and substrate (0.25 nM) is 220 nM at 1 mM Mg^{2+};[8] as such, product yield was low without coacervates (Figure 2A, 2B blue) at only about 5% after 30 min (Figure 2C). Consistent with our previous report[8], in D_{10}/PDAC coacervates substrate cleavage was enhanced compared to buffer (20% vs 5% at 30 min, Figure 2B and C orange). Notably, reaction was further stimulated upon lengthening the anion with D_{30}, D_{50}, and D_{100} in PDAC-containing coacervates (~30% after 30 min) (Figure 2B, and C).

To investigate RNA-partitioning, we used Alexa488-tagged hammerhead substrate and measured fluorescence intensity within droplets. All four polyaspartates formed coacervates with PDAC and accumulated RNA substrate (Figure 2D). We estimated substrate concentration inside coacervates by comparing fluorescence intensity to standards of Alexa488-tagged substrate in the absence of coacervates at various concentrations (Supplementary Figure 1). Although just 0.25 μM labeled substrate was added to the bulk,

droplet substrate concentration was calculated at 106±3, 79±1, 58±3, and 47±1 μM for coacervates containing D_{10}, D_{30}, D_{50}, D_{100} (Figure 2E). This inverse trend is likely due to the tendency of longer polyaspartic acids to interact with coacervate polycations. We conjecture that while short polyanion-containing coacervates (e.g. D_{10}/PDAC) partition HHRz more strongly, RNAs outcompete these short polyanions for interaction with polycation, potentially preventing their catalytic fold. Intermediate polyanions (e.g. D_{50}) decrease RNA partitioning somewhat, but may prevent strong inhibitory RNA-polycation interactions, leading to maximal ribozyme reactions (Figure 2C). Taken together, optimal RNA catalysis in complex coacervate has an ideal polyanion length that requires RNA sequestration without RNA folding interference.

If the influence of polyanion length is based on simple competition with ribozyme for coacervate-polycation, then similar effects should be obtainable by adding relatively short oligoanions (Figure 3). We therefore varied the amount of oligoanion $D_{10,}$ keeping the total positive charge from PDAC constant such that the ratio of total negative to total positive charge increased as 0.5:1, 1:1, 2:1, 3:1, and 5:1 (Figure 3B). Relative to 1:1 (−/+), product was enhanced ~two-fold at 3:1 (−/+) total charge ratio for D_{10} (Figure 3A and 3B orange). No significant changes in bulk pH were observed under these conditions as assessed by pH measurements using a pH probe. Control reactions showed that increasing D_{10} does not affect coacervate-free reactions, ruling out non-specific effects such as counterions (sodium) driving rate enhancements (Supplementary Figure 2). Moving to longer polyanions, increasing the concentration of D_{30} gave a slight bell-shaped dependence but had little effect even up to 50 mM total negative charge (Figure 3B). However, for D_{50}, 50 mM total negative charge reduced the ribozyme activity almost 4-fold (Figure 3B). In the case of D_{100}, ribozyme activity was severely diminished, even with only 20 mM total negative charge (Figure 3B). These data reveal that competition from short polyanions significantly enhances RNA functions in complex coacervates, while competition by long polyanions has the opposite effect.

We next investigated effects of increasing polyanion concentration on RNA partitioning. Increasing the negative:positive charge ratio in D_{10}/PDAC from 1:1 to 5:1 reduced partitioning of the HHRz substrate ~2-fold (Figure 3C boxes 1–3, Figure 3D orange). In coacervates containing 5:1 D_{30}/PDAC and D_{50}/PDAC, substrate concentration further decreased from 70 μM in D_{10} to 14 and 3 μM, respectively (Figure 3C boxes 6 and 9, Figure 3D 5:1). Coacervates containing 5:1 D_{50}/PDAC were almost indistinguishable from background (Figure 3C box 9). Overall, these data suggest that conditions that favor strong RNA partitioning, such as charge-matched coacervates comprising smaller polyanions (Figure 3C box 1), disfavor ribozyme catalysis (Figure 3B). Large polyanions alleviate these potentially inhibitory ribozymepolycation interactions, but they also reduce RNA partitioning (Figure 3C boxes 5,6,8,9), thus impeding reaction. Favorable conditions can be attained by competing strong RNA-coacervate interactions by adding shorter polyanions (Figure 3C boxes 2,3), which still have appreciable RNA partitioning for faster ribozyme reaction (Figure 3D, 3B orange). Overall, these data provide mechanistic insights into facilitation of ribozyme reactions in complex coacervates.

The fluorescence-based assay reports only on the 22-nt substrate strand; we thus compared effects of increasing polyanion concentration on the larger 46-nt ribozyme to the 22-nt substrate. Greater than 90% of the substrate and 97% of the ribozyme remained in the condensed phase at 1:1 D_{10}/PDAC or D_{50}/PDAC coacervate system (Supplementary Figure 3 A–C). At 5:1 D_{10}/PDAC, about 74% of the substrate (Supplementary Figure 3B) and 95% of the ribozyme remained in the condensed phase. However, the amount of substrate in the condensed phase decreased to just 24% at 5:1 D_{50}/PDAC (Supplementary Figure 3C) while about 75% of the ribozyme remained in the condensed phase. Overall, partitioning of longer RNA is less-sensitive to competition from longer polyanions. This can be understood in light of the relative multivalency of the RNAs as compared with the polyanions with which they compete for polycation binding.

To test the generality of our findings to other ribozyme systems, we used the hairpin ribozyme shown in (Supplementary Figure 4A). Unlike the hammerhead ribozyme, where the substrate is extensively base-paired to the enzyme strand, the substrate in the hairpin ribozyme is part of a separate domain, which is recognized via tertiary interactions by the catalytic strand. At low concentrations of Mg^{2+} and ribozyme, coacervates made using D_{30}/(PDAC+spermine) stimulate the reaction[8]. In the absence of coacervates the product yield was only about 10% (Supplementary Figure 4B). The product yield decreased two-fold to 5% in D_{30}/(PDAC+spermine) coacervates at 0.5:1 (−/+) total charge ratio, suggesting that excess polycation is inhibitory, presumably due to misfolding of ribozyme due to strong RNA-polycation interactions. Notably, the product yield increased four-fold to 20% in coacervates with 1:1 (−/+) D_{30}/(PDAC+spermine), which is likely due to release of strong ribozymepolycation interactions. Increasing the total negative charge further had no stimulatory effect. These data support the conclusion that polyanion-assisted stimulation of ribozyme activity can be applied to different ribozymes and that optimal −/+ ratio likely depend on the ribozyme system.

In principle, the ion-pairing model should be applicable to other polyanions. To test this, we compared D_{30} with alternative non-biological polycarboxylates polyacrylic acid (PAA_{25}) and polymethacrylic acid ($PmAA_{45}$), with approximately 25 and 45 negative charges per molecule, respectively (Figure 4). At 1:1 charge balance, all the tested polyanions formed condensed phases with PDAC (Figure 4A). The concentration of Alexa488-tagged HHRz substrate in D_{30}/PDAC, PAA_{25}/PDAC, and $PmAA_{45}$/PDAC coacervates was 80±2, 72±2, and 55±5 μM, respectively (Figure 4A and Supplementary Figure 5A) indicating that all coacervate compositions partition the substrate effectively.

Upon investigation of the HHRz reaction in these different polycarboxylate-containing coacervates, we found that the reaction was optimal in D_{30}/PDAC and $PmAA_{45}$/PDAC coacervates (Figure 3B green and blue and Supplementary Figure 5B), while the product formed was reduced 5-fold in PAA_{25}/PDAC (Figure 4B, dashed orange). Increased activity in $PmAA_{45}$ compared to PAA_{25} (~49% vs 8% at 30 min), parallels the phenomenon observed with D_n as a function of length. Increasing total negative charge in PAA_{25}/PDAC system to 2:1 (−/+) (Figure 4B light orange and Supplementary Figure 5C) partially restored the reaction (~17% vs 8% after 30 mins), similar to D_{10}/PDAC system (Figure 4B). Strikingly, at 3:1 (−/+) charge ratio, the reaction was inhibited in PAA_{25}/PDAC

system (Figure 4B dark orange). Indeed, at 3:1(−/+) charge ratio, the coacervate droplets became almost indistinguishable from background while coacervate droplets with 1:1 and 2:1 (−/+) charge ratios were fluorescent (Supplementary Figure 5D), suggesting similar mechanisms for ribozyme inhibition and activation as observed with oligoaspartic acid and PDAC-containing coacervates (Figure 3). To further test if the stimulatory effect of polyanions is general, we asked whether oligoRNA (rA11) and heparin, which are biogenic polyanions that contain phosphates or carboxylates and sulfates, respectively, can stimulate ribozyme reaction by competition, similar to D_{10}. We first formed complex coacervates with D_{10}/PDAC at 1:1 charge balance, then added excess D_{10}, rA11, or heparin such that the final −/+ total charge was 1.5:1. Under these conditions, addition of both rA11 and heparin increased the product yield to comparable levels as excess D_{10} (Figure 4C). Overall, these data show that coacervates containing both biogenic and abiogenic polyanions enhance ribozyme catalysis. These studies provide rules for enhancing HHRz activity by controlling polyanion length and concentration, which transfer to diverse polyanions. The ability of diverse polyanions to stimulate ribozyme catalysis in membraneless compartments of complex coacervates underscores the power of enhancing RNA-catalyzed reactions in complex coacervates. (total −/+). Indicated polyanions were added to make the total charge balance 1.5:1 (total −/+). Mean values of three replicates are shown; error bars represent the S.D.

For experiments in the preceding sections, PDAC was used as the polycation. We next sought to apply our understanding to coacervates formed with the biogenic and more inhibitory polycation, oligoarginine. We previously reported that coacervates made with D_{10}/R_{10} at charge-matched conditions inhibit HHRz reaction.[8] While PDAC engages only in long-range charge-charge contacts, oligoarginine can engage with RNA in short-range charge-charge and hydrogen-bonding interactions,[22, 23] which can misfold RNA. After 90 minutes, fraction product formed by D_{10}/R_{10} coacervates was reduced ~10-fold compared to D_{10}/PDAC coacervates at 1:1 charge-matched condition (Figure 5A and B). However, increasing charge balance to 2:1 D_{10}/R_{10}, increased product yield 6-fold compared to 1:1 D_{10}/R_{10} (Figure 5B compare green to orange). Strikingly, increasing the charge balance to 3:1 D_{10}/R_{10} enhanced product yield 12-fold (Figure 5B). These data demonstrate that excess polyanions can stimulate ribozyme reactions not only in coacervates that already provide enhancements compared to buffer (Figure 3 A and B), but also in coacervate systems that do not otherwise appreciably support ribozyme reactions at charge-matched conditions.

PDAC or R_{10} was held at 10 mM, total negative charge from D_{10} was varied as indicated. Time points are 0, 7.5, 15, 30, 60, and 90 min (B) Fraction of product formed after 90 minutes was normalized to $D_{10/}$ PDAC coacervates. Mean values from n=3; error bars represent the S.D

Polyion multivalency is important in the formation and physical properties of complex coacervates[24]. Our results demonstrated that complex coacervates with varying lengths of biogenic and abiogenic polyanions and polycations can support and enhance ribozyme catalysis. Mechanistic insights that enable productive RNA folding and partitioning leading to active ribozymes in complex coacervates are revealed. Short polyanions stimulated RNA catalysis in otherwise non-compatible complex coacervates. Improvement of ribozyme

reactions by oligoRNA and heparin suggests that the effects observed herein are general. Thus, other physiological polyanions such as nucleotides, RNAs, and functionalized polysaccharides may help to tune the strength of interactions in microenvironments inside intracellular NMCs. Changes in properties of NMCs may affect folding of RNAs inside such condensates. Furthermore, tetramers of oligoaspartic acid and oligoglutamic acid have been observed in potential prebiotic reactions[25] highlighting the relevance of our results in Early-Earth scenarios.

Methods

Reagents:

All chemicals were purchased from Sigma unless specified. Poly(diallyldimethylammonium chloride) 8.5 K (PDAC) (53 monomers) was purchased from Polysciences. Polyaspartic acid with 10, 30, 50 and 100 monomers were purchased from Alamanda Polymers. All polymers were purchased as sodium or chloride salts. Stock solutions were neutralized using HCl or NaOH solutions where needed. All oligonucleotides were purchased from Integrated DNA Technologies. Radioactive [γ-32P] ATP was purchased from Perkin Elmer. Ribozymes were *in vitro* transcribed using dsDNA as templates. 5′ -32P–labelled substrates for ribozymes were generated using using T4 Polynucleotide Kinase (New England Biolabs).

Hammerhead ribozyme reaction in coacervates:

Solutions containing 25 nM ribozyme and 2.5 nM substrate were heated separately at 85°C for 3 minutes in 25 mM Tris pH 8.0 and 2.5 mM KCl. Coacervate solutions were then prepared in 25 mM Tris pH 8.0, 1 mM $MgCl_2$, and 2.5 mM KCl by first adding water, buffer, and polyanions. Coacervation was induced by adding PDAC and polyaspartic acid or other polyanions (polyacrylic acid or polymethacrylic acid) assumed to be fully charged at pH 8.0. Total positive charge from PDAC was held at 10 mM in all experiments. Total negative charge from polyaspartic acid was held at 10 mM for experiments in Figure 2. Varying amounts of total negative charge from polyaspartic acid or polyacrylic acid was used for figures 3, 4, and 5. Once the coacervates were formed, 5 μl of 25 nM ribozyme solution was added followed by addition of the 5 μL of 2.5 nM substrate solution to initiate the reaction (50 μL final volume). Reactions were then immediately aliquoted into different tubes in 5 μL. “Stopping solution” (15 μL) (166 mM EDTA, 8.3 mM polyacrylic acid 1.8 kDa, 30% formamide) was added at 0, 7.5, 15, 30, 60, and 90 min to stop the reactions. Samples were then heated at 90°C for 1.5 min before separating by a 20% denaturing PAGE. Gels were dried and exposed in phosphor screens and scanned using Typhoon FLA 9000 (GE). Images were analyzed in FIJI (FIJI is Just ImageJ). Fraction product formed at indicated times were fit to:

$$f(t) = fmax\left(1 - e^{(-kobs \cdot \mathrm{t})}\right) \quad \text{eq.1}$$

For reactions in Figure 4, D_{10}/PDAC coacervates were formed as described above at 1:1 (−/+) total charge. Oligoaspartic (D10), oligoRNA (rA11) or heparin (3kDa) were added such that the final charge balance was 1.5:1 (−/+).

Substrate concentration in coacervates:

Standards of Alexa-488-labelled substrate were made at 1, 5, 25, 50, 100, and 135 μM in 25 mM Tris pH 8.0, 1 mM $MgCl_2$, 2.5 mM KCl. Samples of coacervates were then prepared as described above in 20 μL. Fluorescently-labelled HHrz substrate was then added at 0.25 μM final bulk concentration. Samples were left to equilibrate for 5 minutes and 10 μL and transferred on a glass coverslip and viewed in the Leica TCS SP5 laser scanning confocal inverted microscope (LSCM) with a 63X objective lens. 488 nm laser was used for excitation and emission spectra were collected from 510 to 550 nm. Leica LAS AF software was used to acquire the images.

Scintillation Counts of ^{32}P RNA:

Samples were prepared with or without coacervates at 1:1 or 5:1 total charge (D_n:PDAC). Total positive charge from PDAC was held at 10 mM. ^{32}P- labeled RNA was added and mixed thoroughly by pipetting. The final volume after the addition of RNA was 20 μL. For solutions that did not undergo centrifugation, 10 μL of the sample was then added to a separate scintillation vial and set aside for measurements. Separately, identical samples were then centrifuged at 14,000xg for 2 minutes, and 10 μL of the supernatant was taken and added to scintillation vials. ^{32}P measurements were taken in Beckman Coulter LS6500 Scintillation counter. Counts were corrected for signal in the 10 μL fraction of samples without complex coacervates that did not undergo centrifugation.

Hairpin ribozyme reaction in coacervates:

Solutions containing 500 nM ribozyme and <1 nM substrate were heated separately at 85°C for 3 minutes in 25 mM Tris pH 7.5, 1.25 mM $MgCl_2$, and 1.25 mM KCl. Coacervate solutions were then prepared in 25 mM Tris pH 7.5, 2.5 mM $MgCl_2$, and 2.5 mM KCl by first adding water, buffer. D_{30} was added such that the total negative charge was 5, 10, 15 and 20 mM. Spermine and PDAC were then added such that the total positive charge was 5 mM each from both polyamines. All polyions were assumed to be fully charged at pH 7.5.

pH measurements:

Coacervates were prepared at indicated −/+ balance in 25 mM Tris pH 8.0, 1 mM $MgCl_2$, and 2.5 mM KCl. Samples were prepared in 300 μL volume in 1.5 mL microfuge tubes. Once all the components were added, pH was measured using a pH meter (VWR).

Supplementary Material

Refer to Web version on PubMed Central for supplementary material.

Acknowledgements:

The authors would like to thank D. Burke-Aguero (University of Missouri) for critical feedback, and members of the Bevilacqua and Keating labs for carefully reading the manuscript.

Funding: This work was supported by Grant 290363 from the Simons Foundation to R.R.P. and NASA Grant 80NSSC17K0034 to P.C.B and C.D.K.

References

[1]. Bungenberg-de Jong HG, and Kruyt HR (1929) Coacervation (partial miscibility in colloid systems), Proc. Koninklijke Nederlandse Akademie Wetenschappen.

[2]. Frankel EA, Bevilacqua PC, and Keating CD (2016) Polyamine/nucleotide coacervates provide strong compartmentalization of Mg^{2+}, nucleotides, and RNA, Langmuir 32, 2041–2049. [PubMed: 26844692]

[3]. Koga S, Williams DS, Perriman AW, and Mann S (2011) Peptide-nucleotide microdroplets as a step towards a membrane-free protocell model, Nat Chem 3, 720–724. [PubMed: 21860462]

[4]. Sokolova E, Spruijt E, Hansen MM, Dubuc E, Groen J, Chokkalingam V, Piruska A, Heus HA, and Huck WT (2013) Enhanced transcription rates in membrane-free protocells formed by coacervation of cell lysate, Proc Natl Acad Sci U S A 110, 11692–11697. [PubMed: 23818642]

[5]. Deng NN, and Huck WTS (2017) Microfluidic formation of monodisperse coacervate organelles in liposomes, Angew Chem Int Ed Engl 56, 9736–9740. [PubMed: 28658517]

[6]. Joyce GF, and Szostak JW (2018) Protocells and RNA self-replication, Cold Spring Harb Perspect Biol 10.

[7]. Poudyal RR, Pir Cakmak F, Keating CD, and Bevilacqua PC (2018) Physical principles and extant biology reveal roles for RNA-containing membraneless compartments in origins of life chemistry, Biochemistry 57, 2509–2519. [PubMed: 29560725]

[8]. Poudyal RR, Guth-Metzler RM, Veenis AJ, Frankel EA, Keating CD, and Bevilacqua PC (2019) Template-directed RNA polymerization and enhanced ribozyme catalysis inside membraneless compartments formed by coacervates, Nat Commun 10, 490. [PubMed: 30700721]

[9]. Drobot B, Iglesias-Artola JM, Le Vay K, Mayr V, Kar M, Kreysing M, Mutschler H, and Tang TD (2018) Compartmentalised RNA catalysis in membrane-free coacervate protocells, Nat Commun 9, 3643. [PubMed: 30194374]

[10]. Shin Y, and Brangwynne CP (2017) Liquid phase condensation in cell physiology and disease, Science 357.

[11]. Li P, Banjade S, Cheng HC, Kim S, Chen B, Guo L, Llaguno M, Hollingsworth JV, King DS, Banani SF, Russo PS, Jiang QX, Nixon BT, and Rosen MK (2012) Phase transitions in the assembly of multivalent signalling proteins, Nature 483, 336–340. [PubMed: 22398450]

[12]. Langdon EM, Qiu Y, Ghanbari Niaki A, McLaughlin GA, Weidmann CA, Gerbich TM, Smith JA, Crutchley JM, Termini CM, Weeks KM, Myong S, and Gladfelter AS (2018) mRNA structure determines specificity of a polyQ-driven phase separation, Science 360, 922–927. [PubMed: 29650703]

[13]. Van Treeck B, Protter DSW, Matheny T, Khong A, Link CD, and Parker R (2018) RNA self-assembly contributes to stress granule formation and defining the stress granule transcriptome, Proc Natl Acad Sci U S A 115, 2734–2739. [PubMed: 29483269]

[14]. Feric M, Vaidya N, Harmon TS, Mitrea DM, Zhu L, Richardson TM, Kriwacki RW, Pappu RV, and Brangwynne CP (2016) Coexisting liquid phases underlie nucleolar subcompartments, Cell 165, 1686–1697. [PubMed: 27212236]

[15]. Gomes E, and Shorter J (2019) The molecular language of membraneless organelles, J Biol Chem 294, 7115–7127. [PubMed: 30045872]

[16]. Sabari BR, Dall'Agnese A, Boija A, Klein IA, Coffey EL, Shrinivas K, Abraham BJ, Hannett NM, Zamudio AV, Manteiga JC, Li CH, Guo YE, Day DS, Schuijers J, Vasile E, Malik S, Hnisz D, Lee TI, Cisse II, Roeder RG, Sharp PA, Chakraborty AK, and Young RA (2018) Coactivator condensation at super-enhancers links phase separation and gene control, Science 361.

[17]. Aumiller WM Jr., Pir Cakmak F, Davis BW, and Keating CD (2016) RNA-based coacervates as a model for membraneless organelles: Formation, properties, and interfacial liposome assembly, Langmuir 32, 10042–10053. [PubMed: 27599198]

[18]. Poudyal RR, Benslimane M, Lokugamage MP, Callaway MK, Staller S, and Burke DH (2017) Selective inactivation of functional rnas by ribozyme-catalyzed covalent modification, ACS Synth Biol 6, 528–534. [PubMed: 28139121]

[19]. Horning DP, and Joyce GF (2016) Amplification of RNA by an RNA polymerase ribozyme, Proc Natl Acad Sci U S A 113, 9786–9791. [PubMed: 27528667]

[20]. Bartel D, and Szostak JW (1993) Isolation of new ribozymes from a large pool of random sequences, Science 261, 1411–1418. [PubMed: 7690155]

[21]. Moretti JE, and Muller UF (2014) A ribozyme that triphosphorylates RNA 5'-hydroxyl groups, Nucleic Acids Res 42, 4767–4778. [PubMed: 24452796]

[22]. Blanco C, Bayas M, Yan F, and Chen IA (2018) Analysis of evolutionarily independent protein-RNA complexes yields a criterion to evaluate the relevance of prebiotic scenarios, Curr Biol 28, 526–537 e525. [PubMed: 29398222]

[23]. Chong PA, Vernon RM, and Forman-Kay JD (2018) RGG/RG motif regions in RNA binding and phase separation, J Mol Biol 430, 4650–4665. [PubMed: 29913160]

[24]. Li L, Srivastava S, Andreev M, Marciel AB, de Pablo JJ, and Tirrell MV (2018) Phase behavior and salt partitioning in polyelectrolyte complex coacervates, Macromolecules 51, 2988–2995.

[25]. Gibard C, Bhowmik S, Karki M, Kim EK, and Krishnamurthy R (2018) Phosphorylation, oligomerization and self-assembly in water under potential prebiotic conditions, Nat Chem 10, 212–217. [PubMed: 29359747]

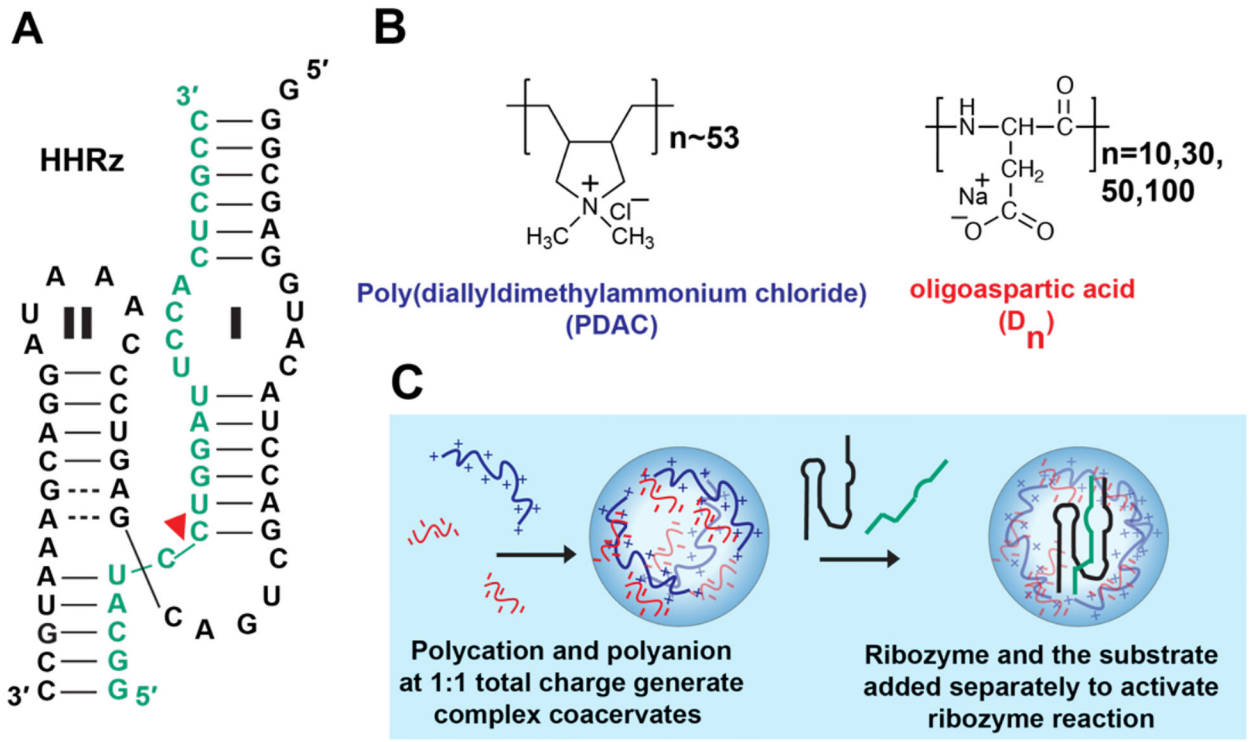

Figure 1.

Hammerhead ribozyme (HHRz) in complex coacervates. (A) Structure of hammerhead ribozyme (black) and substrate (green). Red triangle denotes the cleavage site. Regions involved in tertiary interactions are denoted as I/II. (B) Structures of poly(diallyldimethylammonium chloride) and oligoaspartic acid (D_n, n=10–100). (C) Complex coacervates formed by adding polycation (PDAC) and oligoaspartic acid.

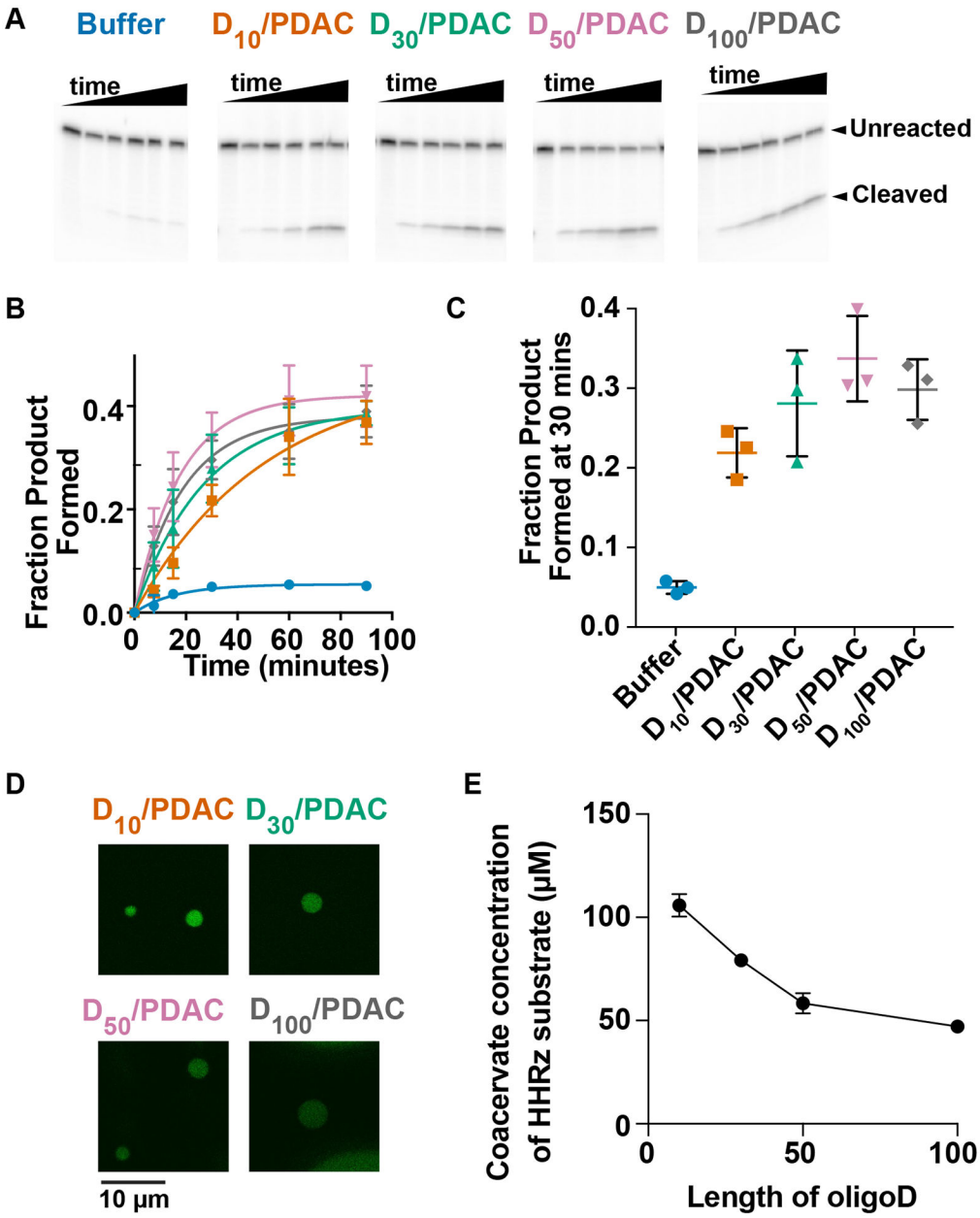

Figure 2.

Polyanion length affects ribozyme catalysis and RNA partitioning. (A, B) Gel images and quantification of HHRz reactions in buffer or coacervates. Reactions were performed in the absence or presence of PDAC-containing coacervates and variable lengths of polyaspartic acid. Time points were taken at 0, 7.5, 15, 30, 60 and 90 min. (C) Fraction product after 30 min. (D) Fluorescence microscopy of coacervates containing 0.25 μM 5'-Alexa-488-tagged HHRz substrate. (E) Calculated concentrations of substrate inside the coacervate. Standard curve is provided in SI Figure 1. Mean values from n=3; error bars represent the S.D

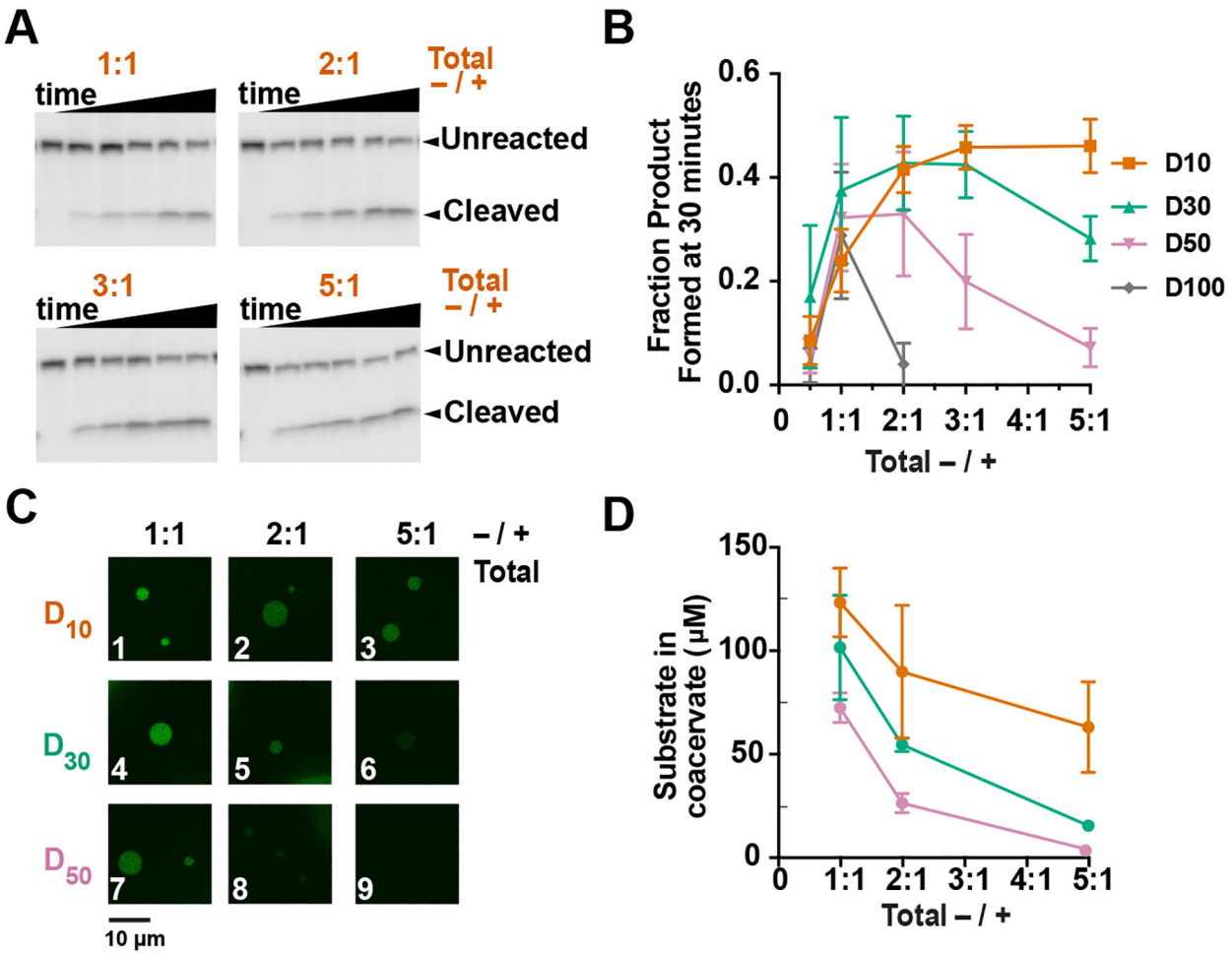

Figure 3.

Excess oligoanions decrease RNA partitioning and enhance ribozyme catalysis. Positive charge from PDAC was 10 mM. (A) Gel images of ribozyme reaction. Total negative charge from D_{10} is 10, 20, 30, and 50 mM to give total −/+ ratios provided above the gels. Time points are 0, 7.5, 15, 30, 60, and 90 min (B) Fraction product formed for coacervates of D_{10}, D_{30}, D_{50}, and D_{100} at 30 min. (C) Confocal microscopy showing partitioning. 0.25 µM Alexa488-labeled HHRz substrate was added to the coacervates. (D) Calculated concentrations of the substrate in coacervates. Mean values of at least three replicates are shown; error bars represent the S.D

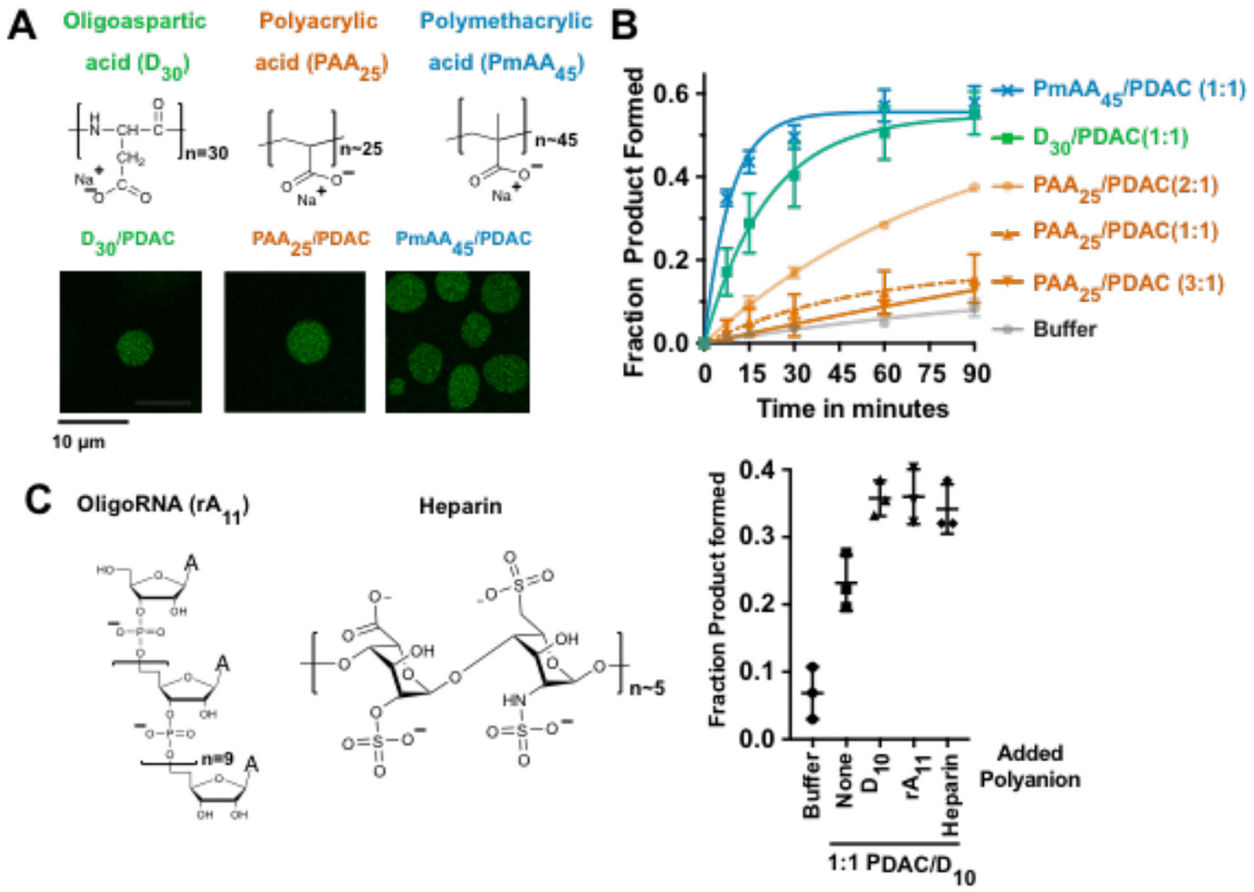

Figure 4.

Diverse polyanions support ribozyme catalysis. (A) Structures of polyanions (top) and images of coacervates in 10 mM PDAC at charge-matched condition (bottom). Oligoaspartic acid (D_{30}) is green, polyacrylic acid (PAA_{25}) is orange, and polymethacrylic acid ($PmAA_{45}$) is blue. Alexa-488-labelled HHRz substrate was added to 0.25 µM. (B) Kinetics of hammerhead cleavage in coacervates containing 10 mM total positive charge from PDAC and total negative charge from different polyanions as indicated. Reaction in the absence of coacervate is gray (buffer). (C) (Left) Structures of heparin and oligoRNA (rA11). (Right) Fraction product formed after 30 min in the absence of coacervates (Buffer) or in coacervates containing D_{10}/PDAC at 1:1

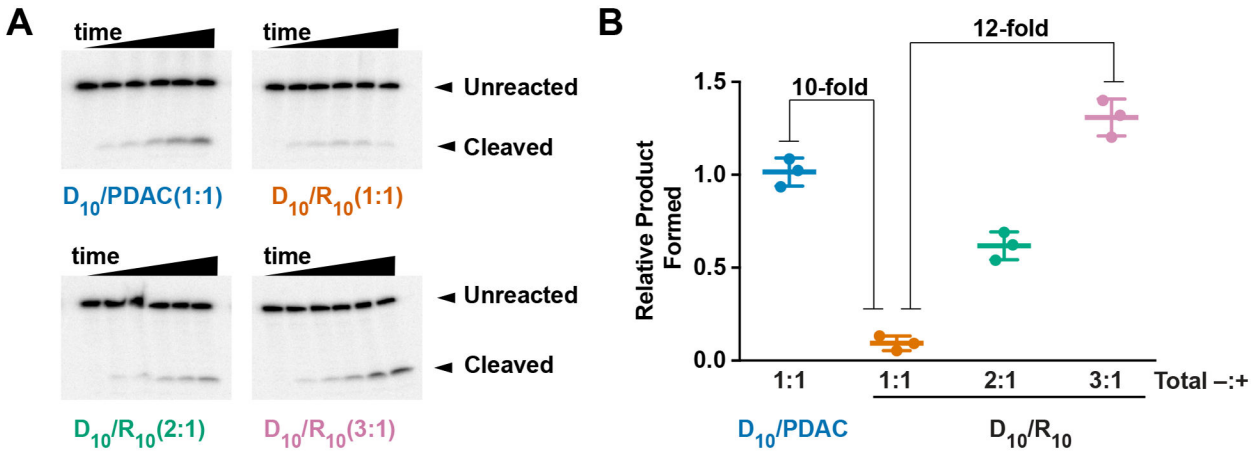

Figure 5.

Polyanions facilitate ribozyme activity in inhibitory coacervates. (A) Gel images showing hammerhead ribozyme cleavage in indicated coacervates. Total positive charge from